AFFINE TRANSFORM RESILIENT ROBUST WATERMARKING TECHNIQUE FOR MEDICAL IMAGES BASED ON IMAGE NORMALIZATION AND SALIENT FEATURE POINTS

Nisar Ahmed Memon *, Asad Ali**, Shaukat Iqbal***

ABSTRACT

To address the issue of copyright protection of medical images in case of affine transformations, we propose a robust image watermarking method using an integrated solution involving moment normalization and salient feature based watermarking in Discrete Cosine Transform domain. First, a new watermarking method based on second generation watermarking concept is proposed. We use salient regions based on Harris feature point detector for watermark embedding and detection process. Second regarding the affine transform attacks, we do not rely upon the normalized disks. We instead use whole image normalization which is resilient to almost all affine transformations such as scaling, translation, rotation, shearing and flipping. The robustness of the approach is verified using both simple and composite affine transformations.

1. INTRODUCTION

The availability of the off-the-shelf image processing software tools in the market has made it easy for hackers and pirates to copy and manipulate the copyrighted digital content. This has increased the threat for digital content owners who use the open networks like internet for transferring their digital assets [4]. New challenges have arisen in the context of easier access and distribution of digital data, especially regarding protection of sensitive medical information. Complementary and/or alternative solutions are nowadays requested in order to confront a number of issues relating to healthcare information management [5]. Millions of medical images are produced daily in radiological departments of the hospitals around the globe. These images are valuable source for both the medical researchers and physicians. This has stimulated continuous expansion and evolution of digital libraries in Medicine, which provide fast and efficient data retrieval from numerous databases in order to foster the creation of new knowledge for medical researchers, and to promote best practice in medical treatment planning for physicians [9]. Consequently information access from these medical image databases raise number of issues that must be addressed, especially those related to security. When a medical practitioner or researcher receives a medical image he/she must be ensured that the image is issued from right source. Thus source authentication of medical images is very important matter relating to health management and distribution [9]. One solution for the protection of medical images is digital image watermarking techniques [6, 8, 9, 10, 24]. The idea is to embed information about the copyright owner into the host image to prevent parties from claiming to be the rightful owners of the data. The watermarks used for that purpose are supposed to be very robust against various attacks intended to remove the watermark [28]. A large number of medical image watermarking techniques [1, 16, 20, 22, 27] been reported in literature for addressing the issue of copyright protection and authentication of medical images. These works are robust to image noise, compression, and spatial filtering, but show severe problems when undergo affine transformations [15]. Affine transformations are also called geometrical distortions and include rotation, scaling translation, cropping, shearing, and projective transformation.

Based on above considerations, we present a blind robust watermarking scheme which is resilient to affine transformations and does not require original image for detection process. The scheme conforms to the strict specifications regarding health data handling by addressing the issue of copyright protection of medical images and preserving their quality and diagnostic value. The scheme embeds the watermark information in the image outside the regions which are important for describes the affine transform resilient watermarking

* Department of Computer Systems Engineering, QUEST, Nawabshah, Pakistan, Email: nisar@quest.edu.pk
** Institute of Industrial Science, University of Tokyo, Tokyo, Japan, Email: asad@iis.u-tokyo.ac.jp
*** Theoretical Plasma Physics Division, PINSTECH, Nilore, Islamabd, Pakistan, Email:shaukat.iqbal.k@gmail.com

approaches. The Concept of feature based watermarking is explained in Section 4. Section 5 explains the proposed scheme and finally experimental results and discussions are described in Section 6.

2. IMAGE NORMALIZATION

In order to cope with the affine transformations introduced in medical images, the image is first normalized in some standard form having the properties of resisting affine transformations. Transforming the image into its standard form requires defining the normalization parameters that are computed from the geometric moments of the image. Let $f(x, y)$ denotes a digital medical image of size $M \times N$, its geometric moments m_{pq} and central moments μ_{pq} for $p, q = 1, 2, 3,...,n$ are defined as:

$$m_{pq} = \sum_{x=0}^{M-1}\sum_{y=0}^{N-1} x^p y^q f(x, y) \tag{1}$$

and

$$\mu_{pq} = \sum_{x=0}^{M-1}\sum_{y=0}^{N-1} (x-\overline{x})^p (y-\overline{y})^q f(x, y) \tag{2}$$

where

$$\overline{x} = \frac{m_{10}}{m_{00}}, \overline{y} = \frac{m_{01}}{m_{00}}$$

Generally an affine transformed image of input image $f(x,y)$ is defined as $G(x_a,y_a)$, where

$$\begin{bmatrix} x_a \\ y_a \end{bmatrix} = A\begin{bmatrix} x \\ y \end{bmatrix} + d \tag{3}$$

provided that det(A) $\neq$ 0. The Equation 3 can also be written as,

$$\begin{bmatrix} x_a \\ y_b \end{bmatrix} = \begin{bmatrix} a_{11} & a_{12} \\ a_{21} & a_{22} \end{bmatrix}\begin{bmatrix} x \\ y \end{bmatrix} + \begin{bmatrix} d_1 \\ d_2 \end{bmatrix} \tag{4}$$

In Equation 4 the matrix A is composite matrix of different affine transformations and is defined as,

$$\begin{bmatrix} x_a \\ y_b \end{bmatrix} = \begin{bmatrix} \cos\theta & -\sin\theta \\ \sin\theta & \cos\theta \end{bmatrix}\begin{bmatrix} \alpha & 1 \\ 1 & \delta \end{bmatrix}\begin{bmatrix} 1 & \beta \\ \gamma & 1 \end{bmatrix}\begin{bmatrix} x \\ y \end{bmatrix} + \begin{bmatrix} d_1 \\ d_2 \end{bmatrix} \tag{5}$$

In Equation 5, the first three matrices on right hand side are called Rotation, Scaling and Shearing matrices, and term after plus sign is called shift or translation vector. The α, δ, β and γ are called transform parameters and are calculated from the image moments by deriving the following results.

Lemma1

If $G(x, y)$ is an affine transformed image of $f(x, y)$ obtained with affine matrix $\begin{bmatrix} a_{11} & a_{12} \\ a_{21} & a_{22} \end{bmatrix}$ and d=0, the following identities hold:

$$m'_{pq} = \sum_{i=0}^{p}\sum_{j=0}^{q}\binom{p}{i}\binom{q}{j} a_{11}^i a_{12}^{p-i} a_{21}^j a_{22}^{q-j} m_{i+j,p+q-i-j} \tag{6}$$

and

$$\mu'_{pq} = \sum_{i=0}^{p}\sum_{j=0}^{q}\binom{p}{i}\binom{q}{j} a_{11}^i a_{12}^{p-i} a_{21}^j a_{22}^{q-j} \mu_{i+j,p+q-i-j} \tag{7}$$

where m'_{pq}, μ'_{pq} are the moments of $G(x, y)$ and m_{pq}, μ_{pq} are the moments of $f(x, y)$.

In our work we adopt the normalization procedure as proposed in [7]. After calculating the transform parameters, the normalization procedure is applied on input medical image which produces the image in some standard form as shown in Figure 1. This standard form of the image always have the same shape even image undergoes simple or composite affine transformations

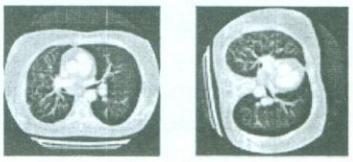

(a) (b)

Figure 1: (a) Original Image (b) Normalized image

3. AFFINE TRANSFORM RESILIENT WATERMARKING APPROACHES

Number of affine transform resilient watermarking approaches is reported in literature. These approaches are roughly divided into four categories:

3.1 INVARIANT DOMAIN-BASED WATERMARKING

In this approach watermarks are embedded and synchronization is maintained in geometric invariant domain. Examples of this type of watermarking are described in [17, 21].

3.2 TEMPLATE-BASED WATERMARKING

In this type of approach additional structured templates are added in frequency domain for identifying geometrical transformations which in turn assisting synchronization. This type of approach is reported in [23].

3.3 MOMENT-BASED WATERMARKING

Geometric moments are employed to normalize the image for maintaining geometric invariance. This type of approach is reported in [2, 3, 12].

3.4 FEATURE-BASED WATERMARKING

In this approach salient regions or object features are utilized for the recovery of geometric attacks. Usually some corner or edge detector such as SIFT, Harris, FAST, SUSAN is used to find the feature points. This approach is reported in [5, 13, 25]. Our proposed method falls in this category.

4. SALIENT FEATURE BASED WATERMARKING

The salient feature-based watermarking is also called content-based image watermarking. This type of watermarking techniques is categorized as second generation watermarking techniques. In this type of watermarking usually feature points are extracted to represent the content of image. Salient points are defined as isolated points in image for which a given saliency function is maximal. The points can be corners or locations of high frequency [26]. In addition points are perceptually significant parts of image and can thus resist various types of common signal processing such as JPEG compression, and geometric distortions. These feature points can also act as marks for (location) synchronization between watermark embedding and detection [25]. In the proposed method we use Harris corner detector [11] as a tool for finding feature points.

5. PROPOSED METHOD

This section describes the proposed method by explaining the embedding and extraction procedures.

5.1 GENERATION OF INVARIANT REGIONS

The proposed method uses Harris feature-based invariant regions to embed the watermark. For this purpose we first normalize the image as described in Section 2 to make the image invariant to rotation, scaling, translation, shearing, and flipping. Harris feature points are then selected from normalized image. In order to detect watermarks without the help of original image, we must look for feature points that are perceptually significant and can resist various image processing operations and desynchronizing attacks. For this purpose we find most stable feature points from a set of detected feature points. For each detected feature point, the search within a circular window whose radius is set to some value say r, is performed. If the detector response R at the feature point achieves local maximum, it is selected as locally most stable point, otherwise it is discarded. Figure 2(a) shows the locally most stable points selected on XRAY medical image. In Figure 2(a), some of the circular windows are overlapping with each other. To obtain non-overlapped patches, the feature point with biggest response say P_{max} in the set of overlapped feature points is chosen and points whose windows overlap with that of P_{max} are then discarded. The procedure for selecting non-overlapped feature points is further discussed in [18]. Figure 2(b) shows the finally selected non-overlapped most stable feature points. It can be observed from Figure 2(b) that some of the stable feature points are lying on the edges of the normalized image. These feature points are vanished when the image is inverse normalized. It is therefore required to discard these feature points too. For this purpose, we use the following procedure. Find the number of black pixels in each circular area, if the number of black pixels is greater than 10% of the total pixels of the circular area it is discarded. Figure 2(c) shows the finally selected feature points used for embedding the watermark.

5.2 BLOCK-BASED EMBEDDING

As mentioned earlier, the proposed method uses feature points for watermark synchronization, therefore

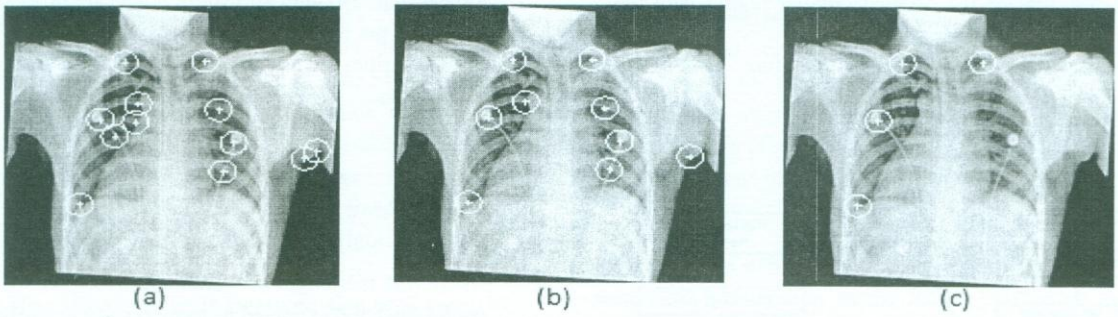

Figure 2: (a) Feature points selected by Harris Corner Detector (b) Non-overlapped Locally most stable points (c) Finally selected feature points

watermark embedding should not affect these feature points. Keeping this point in mind, we propose the block-based DCT-domain embedding instead of full-frame, and leave the middle block of patch without embedding any watermark information. This prevents the neighbouring pixels around the feature point from modification. This helps not only in maintaining the synchronization but also results in accurate recovery of watermark information. Figure 3(a) shows the proposed method of embedding based on block-based embedding in the patch and Figure 3(b) shows the full-frame embedding of patch.

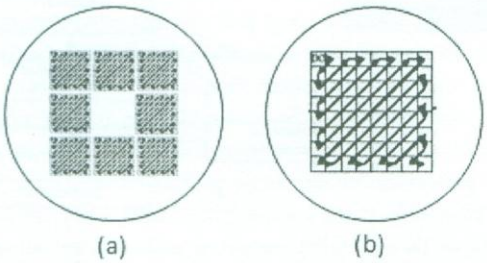

Figure 3: (a) Proposed block-based method of embedding (b) Watermarking embedding method used in [18].

5.3 EMBEDDING PROCEDURE

The block diagram of embedding procedure is shown in Figure 4, and its each step is explained as follows:

1. Normalize the image so that it becomes invariant to affine transformations, as described in Section 2;
2. Apply the Harris corner detector to find the non-overlapped most stable feature points;
3. Extract the rectangular patch from circular region based on each feature point;
4. Divide the rectangular region into nine 8×8 blocks;
5. Divide the watermark into 8 equal parts;
6. Embed each part of the watermark in each block of the patch after transforming it into DCT domain and following the zigzag scan, leaving the middle block unmodified, as shown in Figure 3(a);
7. The embedding is performed by selecting 8 pairs of adjacent coefficients from mid-frequency DCT coefficients in each block;
8. If f_1 and f_2 are DCT coefficients within a pair, and b_i is the watermark bit, then embed the watermark as follows:

   If $b_i = 1$ and $K = f_1 - f_2 < T$, then

   $$f_1^{'} = f_1 + \frac{T-K}{2}$$

   $$f_2^{'} = f_2 - \frac{T-K}{2}$$

   else if $K = f_1 - f_2 > T$, do nothing

   and

   If $b_i = 0$ and $K = f_2 - f_1 < T$, then

   $$f_1^{'} = f_1 - \frac{T-K}{2}$$

   $$f_2^{'} = f_2 + \frac{T-K}{2}$$

   else if $K = f2 - f1 > T$, do nothing;

   Repeat this process for all 8 blocks in rectangular patch;
9. Apply inverse DCT on each block and reconstruct the watermarked rectangular patch;
10. Replace the rectangular patch with the watermarked one in circular region;

11. Finally, replace the original circular region with the watermarked circular region;
12. Repeat steps 4-11 until all feature points are processed.

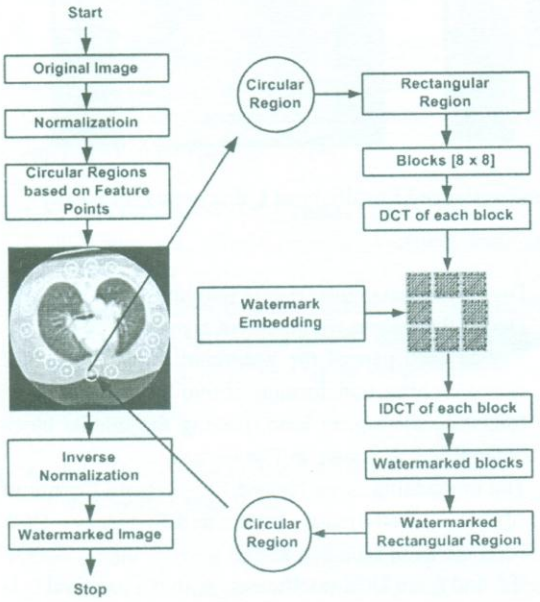

Figure 4: Block diagram of embedding process

5.4 EXTRACTION PROCEDURE

In watermark extraction procedure, first several steps are similar to those of watermark embedding procedure. The block diagram of extraction procedure is shown in Figure 5 and is explained as under:

1. Normalize the image so that it becomes invariant to affine transformations, as described in Section 2;
2. Apply the Harris corner detector to find the non-overlapped most stable feature points;
3. Extract the rectangular patch from circular region based on feature point;
4. Divide the rectangular region into nine 8 × 8 blocks;
5. Extract the watermark information from each block leaving the central block by using the equation;

$$\hat{b}_i = \begin{cases} 1; & f_1' \geq f_2' \\ 0; & f_1' < f_2' \end{cases} \qquad (8)$$

6. Concatenate the watermark information extracted from each block into single watermark $\hat{b}$;
7. Repeat steps 3-6 until all feature points are processed;
8. Calculate the normalized correlation (N_c) to evaluate the similarities between the embedded and extracted watermarks:

$$N_c = \frac{\sum_{i=1}^{n} b(i)\hat{b}(i)}{\sqrt{\sum_{i=1}^{n} b^2(i)}\sqrt{\sum_{i=1}^{n} \hat{b}^2(i)}} \qquad (9)$$

where n is the length of watermark and b and $\hat{b}$ are the original and extracted watermarks respectively;

9. Decide the authenticity of image by considering the maximal N_c value obtained from all the patches.

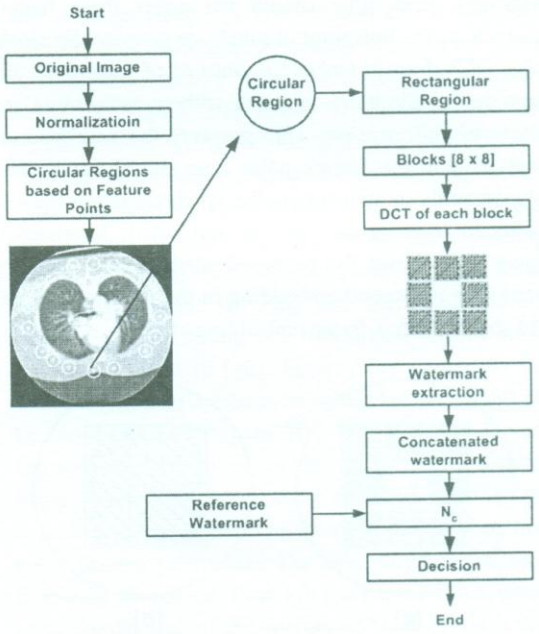

Figure 5: Block diagram of extraction process

6 EXPERIMENTAL RESULTS AND DISCUSSIONS

The concept of affine transform distortions in medical images is new and few works are reported. However, the existing works addressing the issue of the affine transform distortions report results on natural images, we therefore first compare our proposed technique with the existing techniques on standard Lena image and then we report results for medical images.

6.1 RESULTS ON NATURAL IMAGES

In first phase of experiments we apply the proposed algorithm on standard Lena image of size 512 × 512. In order to convey the copyright information in image, a pseudo random binary sequence is generated by using a secret key and this generated sequence is used as watermark. The length of watermark is fixed as 32 bits, which is sufficient for conveying copyright information for a natural image. The distortion introduced in Lena image after watermarking is measured with peak signal to noise ratio (PSNR) and is found 37.07dB. In order to show the robustness of the proposed method a number of geometrical distortions is applied on Lena image. We compare our results with [14] and [18]. The comparative results are shown in Table 1. It can be observed from Table 1, that the proposed method is robust to RST as well composite RST attacks. For rotation attacks our method can tolerate the distortion more than 60 degrees in case of Lena image. The proposed is robust to scaling, even when image is scaled down to more than half of its original size. The method is also robust to composite attacks like rotation followed by scaling, rotation followed by JPEG compression and scaling followed by JPEG compression. In all attacks from S.No. 1 to 28, proposed method performs better than [14] and [18]. This is mainly due to the fact that Lee's scheme embeds the watermark in spatial domain some what like added noise and Li's scheme gives poor response to feature point detector due to embedding on or near to feature point position, whereas the proposed method uses block-based DCT domain watermarking technique for embedding and leaves the block where feature point exists, thus does not allow the modification in feature point as well as in its neighbourhood. We also report the results of horizontal and vertical flipping and number of shearing attacks applied on x-axis, y-axis and combined attacks like rotation followed by shearing, scaling followed by shearing, translation followed by shearing and shearing followed by JPEG compression with different quality factors. These attacks are listed from S.No. 29 to 49 in Table 1. Most of the attacks have N_c greater than 0.7 which reveals the robustness of the proposed method.

6.2 RESULTS ON MEDICAL IMAGES

In the second phase we test the proposed scheme on medical images. The proposed algorithm is not directly applied on medical images due to the following reasons:

1. Medical images are composed of region of interest (ROI) and region of non-interest (RONI). ROI is important for physician for making diagnosis, so its integrity must be maintained during watermark embedding process.
2. The amount of distortion should be as minimum as possible

Keeping these points in mind, we propose to embed the watermark information in the RONI only. Also in the proposed method a small amount of distortion is introduced due interpolation process when we normalize the image before embedding and inverse normalize after embedding. In order to get better tradeoff between the imperceptibility and robustness we use watermark of small size. For medical images we also have used the watermark of same size as for natural images i.e 32 bits. In order to avoid the watermark embedding in region of interest, we take the arbitrary shape for isolating the ROI from RONI. For CT scan images we separate the actual lung parenchyma by segmenting the CT scan image into ROI and RONI. We adopt the segmentation technique proposed in [19] for this purpose. While for other medical images we take the arbitrary circular window with radius equal to 100 pixels. For finding the locally most stable feature points after normalizing the medical image we apply the Harris corner detector with following two methods.

(a) DFS method

In this method we find feature points by applying the Harris Corner detector first and then for maintaining the integrity of ROI, we discard the feature points lying in ROI. This method gives better results for images like MRI, Ultrasound and XRAY. However in case of CT scan images it was found that detector was unable to find feature points on most of the CT Scan images, thus makes the DFS method unsuitable for watermarking the CT scan images. This was due to the fact that the CT scan image contains the lung parenchyma which is highly textured region with clear edges. As Harris corner detector mostly finds corners as feature points, so most of the feature points found were concentrated in region of interest. And as per requirement of RONI embedding if we discard all the feature points lying in ROI, all feature points found by DFS method are vanished from input CT scan image and

ISSN 1665-8607

results in no feature point selected for further embedding. This scenario is shown in Figure 6. In order to overcome this deficiency we proceed for the second method.

(b) SFD method

In this method we isolate the ROI first and then apply the Harris Corner detector for extracting feature points. The

Table 1: Watermark robustness to geometric attacks on Lena Image

S.No.	Type of attack	Normalized Correlation		
		Lee et al. [14]	Li et al. [18]	Proposed
01.	R(1)	0.643	1.000	1.000
02.	R(5)	0.641	1.000	1.000
03.	R(10)	0.600	1.000	1.000
04.	R(15)	0.536	1.000	1.000
05.	R(30)	0.514	0.734	1.000
06.	R(45)	-	-	1.000
07.	R(60)	-	-	1.000
08.	R(75)	-	-	0.930
09.	S(0.2)	-	-	0.516
10.	S(0.3)	-	-	0.645
11.	S(0.5)	-	0.672	0.819
12.	S(0.7)	0.472	1.000	1.000
13.	S(0.9)	0.605	1.000	1.000
14.	S(1.1)	0.606	1.000	1.000
15.	S(1.3)	0.594	1.000	1.000
16.	S(1.5)	0.524	1.000	1.000
17.	S(1.7)	-	-	1.000
18.	S(1.9)	-	-	1.000
19.	T(5)	-	1.000	1.000
20.	T(10)	-	0.820	1.000
21.	R(5)+S(0.8)	-	0.953	0.968
22.	R(10)+S(0.8)	-	0.984	1.000
23.	R(15)+S(0.8)	-	0.969	1.000
24.	R(30)+S(0.8)	-	0.719	0.829
25.	R(10)+JPEG(80)	-	0.953	0.966
26.	R(30)+JPEG(80)	-	0.734	0.876
27.	S(0.8)+JPEG(80)	-	0.891	0.903
28.	S(1.5)+JPEG(80)	-	1.000	1.000
29.	ShX(0.1)	-	-	0.968
30.	ShY(0.1)	-	-	0.933
31.	ShX(0.1)+ShY(0.1)	-	-	0.966
32.	Horizontal Flip	-	-	1.000
33.	Vertical Flip	-	-	1.000
34.	R(10)+ShX(0.1)+ShY(0.1)	-	-	0.852
35.	R(20)+ShX(0.1)+ShY(0.1)	-	-	0.733
36.	R(30)+ShX(0.1)+ShY(0.1)	-	-	0.750
37.	R(10)+ShX(0.2)+ShY(0.2)	-	-	0.859
38.	R(20)+ShX(0.3)+ShY(0.3)	-	-	0.791
39.	S(0.8)+ShX(0.1)+ShY(0.1)	-	-	0.968
40.	S(0.8)+ShX(0.2)+ShY(0.2)	-	-	0.828
41.	S(0.8)+ShX(0.3)+ShY(0.3)	-	-	0.791
42.	T(5)+ShX(0.1)+ShY(0.1)	-	-	0.966
43.	T(10)+ShX(0.2)+ShY(0.2)	-	-	0.870
44.	T(15)+ShX(0.3)+ShY(0.3)	-	-	0.808
45.	ShX(0.1)+JPEG(80)	-	-	0.933
46.	ShY(0.1)+JPEG(80)	-	-	0.866
47.	ShX(0.1)+ShY(0.1)+JPEG(80)	-	-	0.939
48.	ShX(0.2)+ShY(0.2)+JPEG(60)	-	-	0.791
49.	ShX(0.4)+ShY(0.4)+JPEG(90)	-	-	0.800

"-" = Not reported by author, "R" = Rotation, "S" = Scaling, "T" = Translation
"ShX"= Shear on X-axis, "ShY"=Shear on Y-axis

ISSN 1665-8607

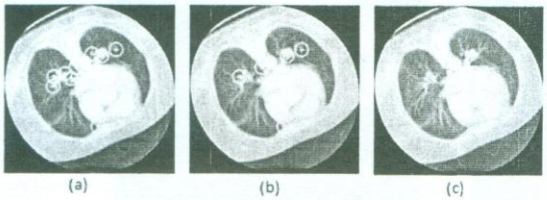

Figure 6: (a) Feature points selected by corner detector on normalized CT scan image (b) Non-overlapped most stable feature points (c) No feature point selected for embedding watermark information.

detailed procedure is defined as under:

1. Mark the logical boundary on the normalized image for isolating ROI;
2. Extend the logical boundary by distance of r, where r is the radius of the circular window;
3. Crop the area bounded by the extended boundary;
4. This will clearly produce the black hole in the image, thus force the detector to find the feature points around the ROI.

The complete cycle of SFD method is depicted in Figure 7.

Figure 8 shows the finally selected feature points for all CT, MRI, Ultrasound and XRAY image by using both DFS and SFD methods. Column 1 in Figure 8 shows the original images, column 2 shows the feature points selected by DFS method and column 3 shows the feature points selected by SFD method. Table 2 shows the number of feature points selected by each method. It can be observed from Table 2, that second method SFD works well and gives assurance of finding sufficient number of feature points for watermarking, every time when it is applied on medical image. We tested the proposed method on CT, MRI, Ultrasound and XRAY images. All images are of size 512 × 512. The value of radius used for circular window is taken as 20 pixels. The watermark length is 32 bits.

Table 2: Locally most stable feature points found by two methods

Image	DFS Method	SFD Method
CT	0	11
MRI	6	13
Ultrasound	7	8
XRAY	4	14

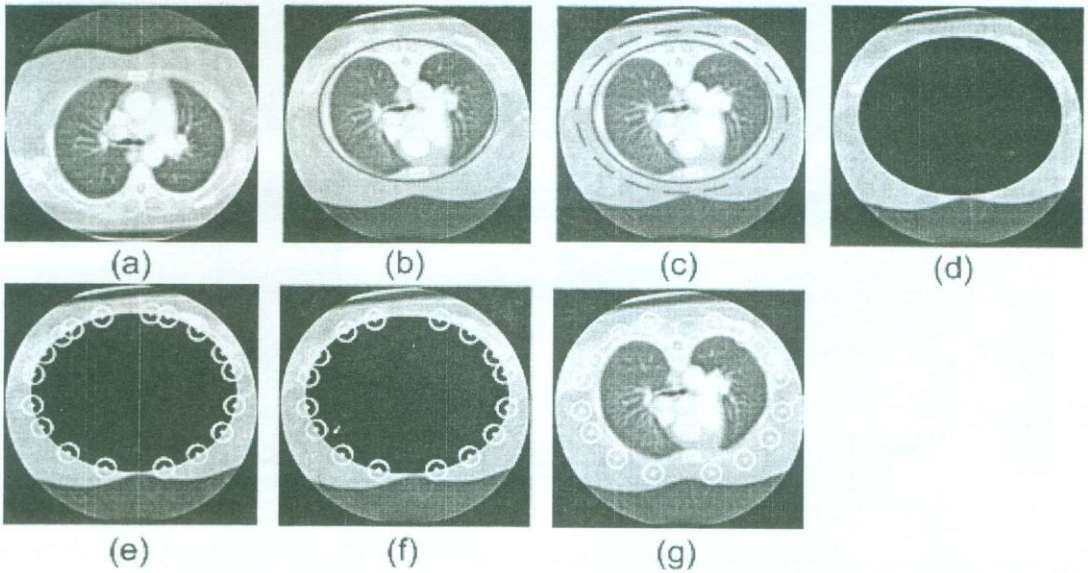

Figure 7: Complete cycle of SFD method: (a) Original image (b) Normalized image with ROI isolated (c) Logical boundary extended (d) Area cropped bounded by extended logical boundary (e) Feature points selected by corner detector (f) Non overlapped feature points selected (g) Finally selected feature points shown on normalized CT scan image

ISSN 1665-8607

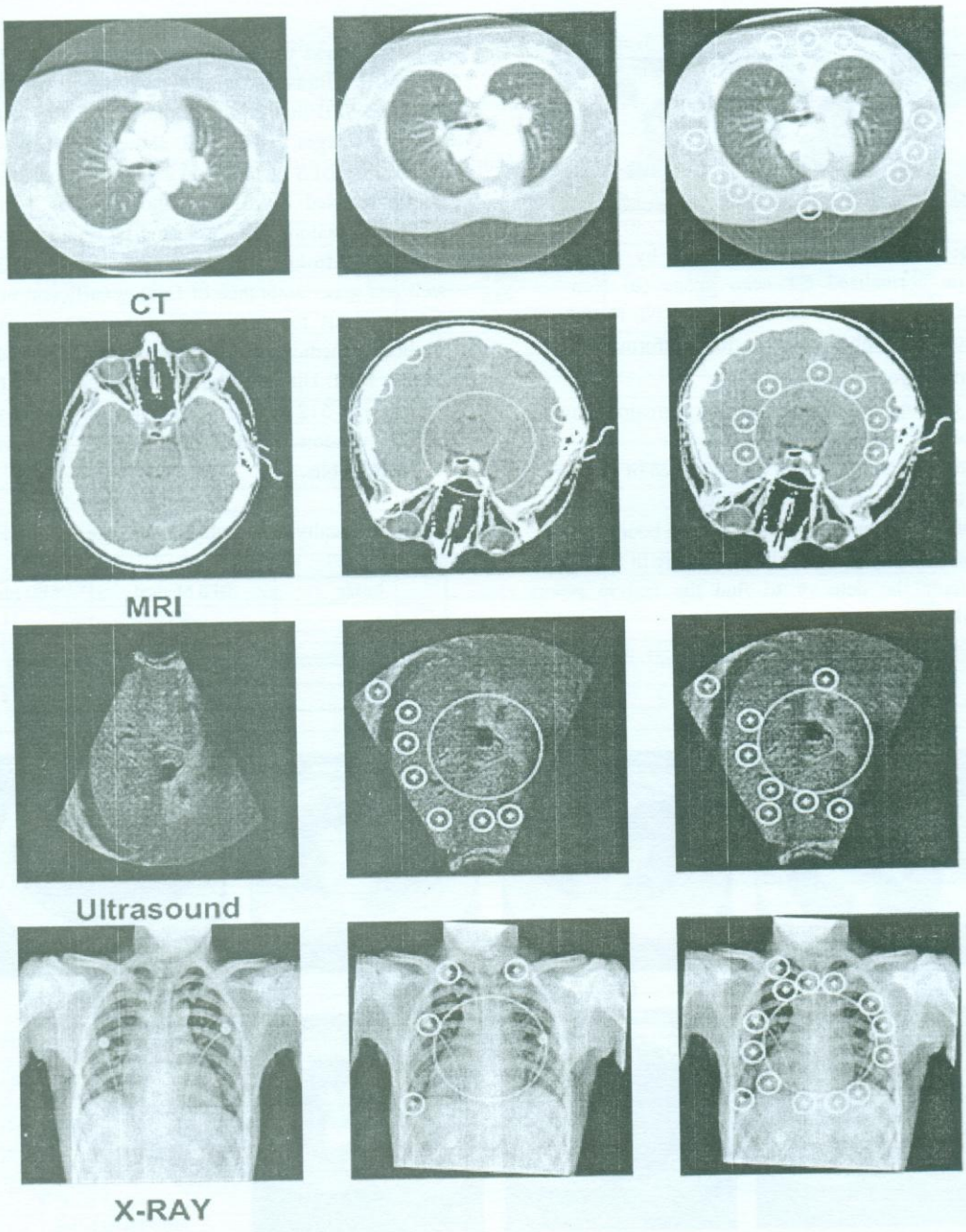

Figure 8: Finally selected feature points by two methods. Column No. 1 shows the original images of CT, MRI, Ultrasound, and XRAY, column No. 2 shows the feature points selected by DFS method and column No. 3 shows the SFD method

The original, watermarked and residual (difference between original and watermarked images) are shown in Figure 9. The distortion introduced in images is measured by using the Peak Signal to Noise Ratio (PSNR). Table 3 shows the values of PSNR for each image. All images have PSNR values greater than 40dB which shows the good imperceptibility of watermarked images.

Table 3: Distortion introduced in cover images after watermarking in terms of PSNR(dB)

Image	PSNR(dB)
CT	45.4449
MRI	47.7396
Ultrasound	49.0673
XRAY	45.9373

In order to show the robustness of the proposed scheme against affine transformations a number of attacks is performed using simple and composite attacks on CT, MRI, Ultrasound and X-ray medical images. The results are tabulated in Table 4 and Table 5. It can be observed from Table 4, that when no attack is performed, the proposed method extracts the watermark accurately. For rotation attacks up to 30 degree most values of normalized correlation are higher than 0.8. The proposed method is robust to scaling, even when the watermarked image is scaled down to 75% of the original size. When the image is zoomed in, most similarities are equal to one or near to 1. This is because when the image is zoomed in, little information is lost. The scheme is also robust to translation attacks. The proposed method is also robust to shearing attacks. From Table 5, we can observe that if we shear the image either on x-axis or y-axis or on both x-axis and y-axis simultaneously up to shearing ratio of 0.1, most similarities are equal to 1. The scheme is also robust to combined attacks such as rotation plus shearing, scaling plus shearing, translation plus shearing.

7. CONCLUSIONS

A blind robust watermarking method based on feature point watermarking and image normalization technique is proposed for the copyright of medical images. Several invariant regions are extracted for conveying the copyright information. Initially image is normalized to make it invariant against geometric distortions and other affine transformations. The circular regions are then extracted from the normalized image. On the basis of invariant regions robust watermarking technique is designed. DCT domain is used for both watermark embedding and extraction. The proposed method address the issue of affine transformations such as shearing, flipping and composite attacks of all affine transformations beside the basic transformations like rotation, scaling and translation.

Table 4: Watermark robustness to geometric attacks medical images

Type of attack	Normalized Correlation			
	CT	MRI	Ultrasound	XRAY
No attack	1.0000	1.0000	1.0000	1.0000
R(1)	1.0000	0.9682	1.0000	0.9682
R(5)	1.0000	0.9682	1.0000	1.0000
R(10)	1.0000	0.9393	0.9682	1.0000
R(15)	1.0000	0.9037	0.9333	0.9333
R(30)	1.0000	0.8391	0.8593	0.8120
R(45)	0.8767	0.7591	0.6000	0.7112
R(60)	0.7912	0.6888	0.4900	0.5010
R(75)	0.6901	0.4521	0.3912	0.4210
S(0.2)	0.5809	0.5333	0.3330	0.5331
S(0.3)	0.5923	0.6055	0.4667	0.5333
S(0.5)	0.7333	0.6516	0.6888	0.6888
S(0.7)	0.9393	0.8767	0.8281	0.7912
S(0.9)	1.0000	0.9837	0.9500	1.0000
S(1.1)	1.0000	1.0000	0.9801	1.0000
S(1.3)	1.0000	1.0000	1.0000	1.0000
S(1.5)	0.8281	0.9333	0.9333	0.9661
S(1.7)	0.8787	0.8520	0.7201	0.7515
S(1.9)	0.7912	0.7000	0.6624	0.7100
T(5)	1.0000	1.0000	1.0000	1.0000
T(10)	1.0000	1.0000	1.0000	1.0000
R(5)+S(0.8)	0.9393	0.8971	0.8767	0.9661
R(10)+S(0.8)	1.0000	0.9837	0.9037	0.7591
R(15)+S(0.8)	0.9661	0.9129	0.9393	0.9682
R(30)+S(0.8)	0.8767	0.8667	0.8391	0.7810

Table 5: Watermark robustness to geometric attacks on medical images

Type of attack	Normalized Correlation			
	CT	MRI	Ultrasound	XRAY
R(10)+JPEG(80)	0.7515	0.7100	0.6445	0.6086
R(30)+JPEG(80)	0.7303	0.5923	0.6351	0.5196
S(0.8)+JPEG(80)	0.6055	0.6694	0.6211	0.5023
S(1.5)+JPEG(80)	1.0000	0.8520	0.9666	0.9682
ShX(0.1)	0.9333	1.0000	0.9393	1.0000
ShY(0.1)	1.0000	1.0000	1.0000	1.0000
ShX(0.1)+ShY(0.1)	1.0000	1.0000	0.9393	1.0000
Vertical Flip	1.0000	1.0000	1.0000	1.0000
Horizontal Flip	1.0000	1.0000	1.0000	1.0000
R(10)+ShX(0.1)+ShY(0.1)	0.9682	0.9333	0.8767	1.0000
R(20)+ShX(0.1)+ShY(0.1)	1.0000	1.0000	1.0000	1.0000
R(30)+ShX(0.1)+ShY(0.1)	1.0000	1.0000	1.0000	1.0000
R(10)+ShX(0.2)+ShY(0.2)	1.0000	1.0000	0.9037	1.0000
R(20)+ShX(0.3)+ShY(0.3)	0.8667	0.8885	0.8767	1.0000
S(0.8)+ShX(0.1)+ShY(0.1)	0.9682	0.9682	0.8971	0.9682
S(0.8)+ShX(0.2)+ShY(0.2)	0.9227	0.8767	0.6901	0.8520
S(0.8)+ShX(0.3)+ShY(0.3)	0.8667	0.7108	0.7303	0.5505
T(5)+ShX(0.1)+ShY(0.1)	1.0000	1.0000	0.9393	1.0000
T(10)+ShX(0.2)+ShY(0.2)	0.9037	1.0000	0.8767	0.8971
T(15)+ShX(0.3)+ShY(0.3)	1.0000	0.9037	0.8944	0.8293
ShX(0.1)+JPEG(80)	0.7006	0.7100	0.6761	0.7515
ShY(0.1)+JPEG(80)	0.7100	0.6888	0.5774	0.7100
ShX(0.1)+ShY(0.1)+JPEG(80)	0.7156	0.6761	0.6262	0.6000
ShX(0.2)+ShY(0.2)+JPEG(80)	0.6901	0.5164	0.4146	0.5022
ShX(0.3)+ShY(0.3)+JPEG(80)	0.5899	0.5477	0.5477	0.5636

ISSN 1665-8607

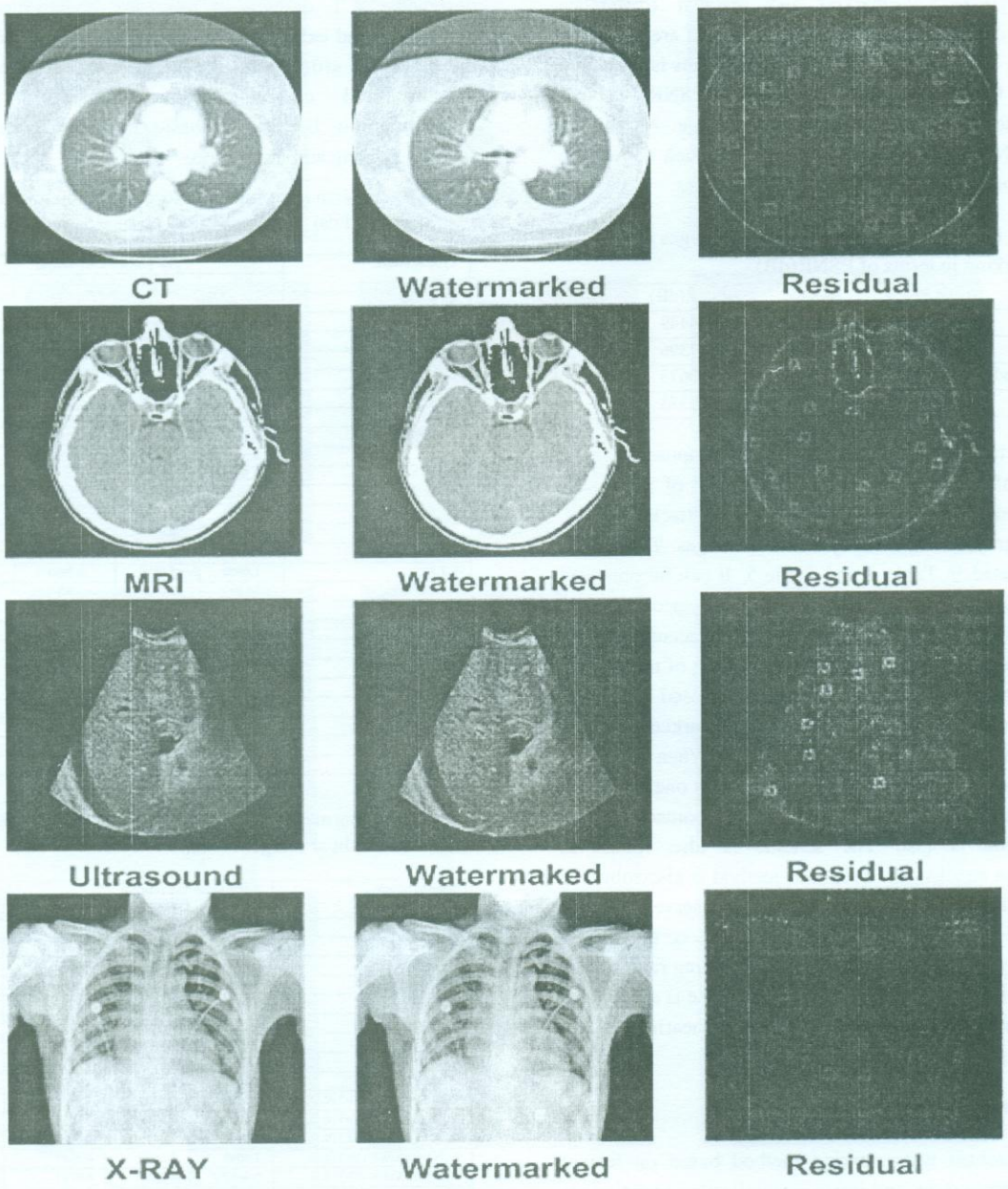

Figure 9: From Left to Right: column 1 shows the original images, column 2 shows the watermarked images and column 3 shows the residual images (difference between original and watermarked images).

In order to maintain the integrity of ROI of a medical image, ROI is avoided from embedding the watermark. The proposed method finds the place in the medical data management, where geometric distortions are of great concern. However one limitation of the proposed method is the introduction of small amount of distortions produced due to interpolation errors when we normalize and inverse normalize the image during watermarking process. Though ROI is prevented during the watermark embedding process, the interpolation errors still can cause distortion in the ROI. One method for avoiding such type of distortions can be the introduction of the improved methods of interpolation which can avoid the interpolation errors in ROI and result in better quality of watermarked image.

ACKNOWLEDGEMENT

Authors are very grateful to Ghulam Ishq Khan Instiute of Engineering Sciences and Technology, Topi, Swabi, Pakistan for providing resources and environment for carrying out this research. Image databases were provided by AGA Khan Medical University Hospital, Karachi, Pakistan. This work was supported by Quaid-e-Awam University of Engineering, Science and Technology, Nawabshah, Sindh, Pakistan under Inland Scholarship programme.

REFERENCES

[1] U. R. Achariya, P. S. Bhat, S. Kumar, L. C. Min, "Transmission and storage of medical images with patient information", Journal of Computers in Biology and Medicine, vol. 33, pp. 303-310, 2003.

[2] M. Alghoniomy, A. H. Twefik, "Image watermarking by moment invariants", Proceedings IEEE International Conference on Image Processing, vol. 2, pp. 73-76, 2000.

[3] M. Alghoniomy, A. H. Twefik, "Geometric invariance in image watermarking", IEEE Transactions on Image Processing, vol. 13, No. 2, pp. 145-153, 2004.

[4] P. Bas, J.-M. Chassery, B. Macq, "Geometrically invariant watermarking using feature points", IEEE Transactions on Image Processing, vol 11, pp. 1014-1028, 2002.

[5] S. Battacharjee, M. Kutter, "Compression tolerance image authentication", Proceedings of IEEE International Conference on Image Processing, vol. 1, pp. 435-439, 1998.

[6] R. R. Colin, C. F. Uribe, J.-A. M. Villanueva, "Robust watermarking scheme applied to radiological medical images", IEICE Transactions on Information and Systems (Letter), vol. E91-D, No.3. , 2008.

[7] P. Dong, J. G. Brankov, N. P. Galatsanos, Y. Yang, F. Davoine, "Digital watermarking robust to geometric distortions", IEEE Transactions on Image Processing 14(12), 2140-2150. 2005.

[8] A. Giakoumaki, S. Pavlopoulos, D. Koutsouris, "Multiple digital watermarking applied to medical imaging", Proceedings of the IEEE 27th Annual Conference on Engineering in Medicine and Biology, Shanghai, China, vol. 4, pp. 3444-3447. 2005.

[9] A. Giakoumaki, S. Pavlopoulos, D. Koutsouris, "Multiple image watermarking applied to health information management", IEEE Transactions on Information Technology in Biomedicine, vol. 10, No. 4, pp. 722-732, 2004.

[10] G. Goatrieux, J. Montagner, H. Juang, C. Roux, "Mixed reversible and RONI watermarking for medical image reliability protection", Proceedings of IEEE 29th Annual Conference of EMBS, Cite Internationale, Lyon, France, vol. 27, pp. 5654-5657. 2007.

[11] C. Harris, M. Stephens, "A combined corner and edge detector", Proceedings of the Fourth Alvey Vision Conference, Manchester, UK, pp. 147-151, 1998.

[12] H. S. Kim, H. K. Lee, 2003. Invariant image watermarking using zernike moements. IEEE Transactions on Circuits and Systems for Video Technology 13(8), 766-775, 2003.

[13] M. Kutter, S. K. Battacharjee, T. Ebrahimi, "Towards second generation watermarking schemes", Proceedings of IEEE Conference on Image Processing, vol. 1, pp. 320-323, 1999.

[14] H.-Y. Lee, H. Kim, H.-K. Lee, "Robust image watermarking using local invariant features", Optical Engineering, vol. 45, No. 3, pp. 1-11, 2006.

[15] H.-Y. Lee, J.-T. Kim, H.-K. Lee, Y.-H, Suh, "Content-based synchronization using the local invariant feature for robust watermarking", Proceedings of C.H. Lim and M. Yung(Eds.),WISA 2004, Springer LNCS 3325, pp. 122-134. 2004.

[16] M. Li, R. Poovendran, S. Narayanan, "Protecting patient privacy against unauthorized release of medical images in a group communication environment", Journal of Computerized Medical Imaging and Graphics, vol. 29, pp. 367-383, 2005.

[17] C. Y. Lin, M. Wu, T. A. Bloom, I, J. Cox, M. L. Miller, Y. M. Lui, "Rotation, scale and translation resilient watermarking of images", IEEE Transactions on Image Processing, vol. 10, No. 5, pp. 767-782, 2001.

[18] L.-D. Li, B.-L. Guo, L. Guo, "Rotation, scaling and translation invariant image watermarking using feature points", The Journal of China Universities of Posts and Telecommunications, vol. 15, No. 2, pp. 82-87, 2008.

[19] N. A. Memon, A. M. Mirza, S. A. M. Gilani, "Segmentation of lungs from CT scan images for early diagnosis of lung cancer", Proceedings of 2006 Enformatika XIV International Conference, Prague, Czech Republic, vol. 14, pp. 228-233, 2006.

[20] H. Munch, E. Engelmann, A. Schroeter, H. P. Meinzer, "Web-based Distribution of radiological images from PACS to EPR", International Congress Series, vol. 1256, pp. 73-879, 2003.

[21] J. J. K. O'Ruanaidh, T. Pun, "Rotation, scale and translation invariant spread spectrum digital image watermarking", Signal Processing, vol. 66, No. 3, pp. 303-317, 1998.

[22] G.-T. Oh, Y.-B. Lee, S.-J. Yeom,, "Security mechanism for medical image information on PACS using invisible watermark", Proceedings of M. Dayde etl al. (Eds) VECPAR 2004, Springer LNCS, vol. 3402, pp. 315-324. , 2005.

[23] S. Pereira, T. Pun, "Robust template matching for affine resilient image watermarks", IEEE Transactions on Image Processing 9(6), 1123-1129, 2000.

[24] F. Y. Shih, Y.-T. Wu, "Robust watermarking and compression for medical images based on genetic algorithms", Information Sciences Elsevier, vol. 175, pp. 200-216. 2005.

[25] C. W. Tang, H. M. Hang, "A feature based robust digital image watermarking scheme", IEEE Transactions on Signal Processing, vol. 51, No. 4, pp. 950-959, 2003.

[26] C. Wu, R. Cathey, "Digital image watermarking: A comparative overview of several digital watermarking schemes", available www.csam.iit.edu/cs549/cs549/presentation report.pdf, 2002.

[27] J. H. K. Wu, R.-F. Chang, C.-J. Chen, C.-L. Wang, T.-H. Kuo, W. K. Moon, R. Chen, "Tamper detection and recovery for medical images using near lossless information hiding techniques", Journal of Digital Imaging, vol. 21, No. 1, pp. 59-76, 2008.

[28] D. Zheng, Y. Liu, J. Zhao, A. E. Saddik, "A survey of RST invariant image watermarking algorithms", ACM Computing Surveys, vol. 39, No. 2, Article 5, 2007.